Available free online at www.medjchem.com

Mediterranean Journal of Chemistry **2013**, 2(4), 595-606

Catalytic oxidation of methanol on Pt/X (X = CaTP, NaTP) electrodes in sulfuric acid solution

Naima Farfour, Mohamed El Mahi Chbihi, Driss Takky, Khadija Eddahaoui and Said Benmokhtar*

LCPM, Laboratory of Chemistry and Physics of Materials, Department of Chemistry, Faculty of Sciences, University Hassan II-Mohammedia, Cdt Driss El Harti, PO Box 7955, Sidi Othman Casablanca, Morocco

Abstract: In this paper, we report the synthesis and characterization of electrodes based on NASICON type phosphates. The study of the electrochemical oxidation of methanol at ambient temperature on electrodes based on NASICON type $Ca_{0,5}Ti_2(PO_4)_3$ (CaTP) and $Na_5Ti(PO_4)_3$ (NaTP) compared to that of the platinum electrode model has been conducted by cyclic voltammetry in acidic medium. The results showed a significant increase of current density on the electro oxidation of methanol on the material developed based NASICON structure CaTP, cons deactivation of the electro oxidation is observed the closed structure type NaTP.

Keywords: Methanol, electrooxidation, electrocatalytic properties, Nasicon, Cyclic Voltammogram.

Introduction

Fuel cells have been projected as promising energy devices responding to the world's increasing demand of safe, eco-friendly and noiseless energy sources[1-3]. In this context, direct alcohol fuel cells, employing, e.g., methanol as a fuel, have received a considerable attention[4] in view of its virtues, e.g., high solubility in aqueous electrolytes, easy handling, transport and storage in comparison with hydrogen gas as a fuel. Moreover, methanol has a high theoretical density of energy (6 kWh kg^{-1}) which is comparable to that of gasoline (10-11 kWh kg^{-1})[5-8].

The electrooxidation of methanol at the Pt electrode is a complex reaction which brings about the formation of a variety of adsorbed intermediates and/or poisons such as CO[9-12], which blocks the active Pt sites and thus causes a significant deterioration of its catalytic activity. The formation of adsorbed intermediates such as CO on the Pt surface results in a methanol oxidation renders the unmodified Pt electrode incapable of oxidizing methanol at a satisfactory rate at a sufficiently low potential. In this context, several modifications of the Pt electrode have been reported in order to mitigate such a poisoning effect aiming at the enhancement of methanol oxidation by increasing the anode tolerance against the reaction intermediates (particularly the poisoning adsorbed CO).

Recently major developments in this area have been prompted by the introduction of foreign metal atoms such as M = Rh, Ru, Sn, Mo or Au[5,13-16] onto electrode surfaces to obtain

**Corresponding author:*

E-mail address: sbenmokhtar@yahoo.com

DOI: http://dx.doi.org/10.13171/mjc.2.4.2013.12.10.23

a suitable replacement for Pt which readily forms surface oxides that can facilitate the complete oxidation of CH_3OH to CO_2[17].

It has been found that Pt-M alloy catalysts generally have high activity, which was attributed to the ability of the M in the alloys to form active oxygen species (-OH) at low electrode potentials (~0.2 V) that can remove poisonous carbon monoxide on the Pt sites[18,19]. The enhanced activity was also attributed to the change of electronic structures of Pt when the more electronegative M is alloyed[20-21]. It was also observed that the distributions of Pt and M sites at the atomic level can substantially affect the catalyst activity. Moreover, Pt electrodes modified with metal oxide (e.g., MoO_3, TiO_2, CeO_2, SnO_2 or Nb_2O_5) have been reported as possible anodes for methanol and CO oxidation reactions[22-28], in which the activity of the modified Pt catalyst towards methanol oxidation is significantly improved. Also several non platinum metals have recently been investigated as electrocatalysts for methanol/ethanol oxidation reaction in alkaline media. NASICON (Na Super Ion Conductor) ceramic electrode is attracting as cathode-active material[29-30], NASICON had a long research history of 20 years as a solid electrolyte. Many interesting cathodes have been proposed based on the NASICON material group, represented as general formula $Li_xM_2(XO_4)_3$ (M= Fe, Mn, Ti, V, Nb, X = S, P, Mo, W, As Si, ….)[31-33]. The features of NASICON cathodes can be summarized as follows, high diffusivity through the large bottleneck due to a shared 3D corner framework (O-X-O-M-O-X-O-), large multiple guest accommodation sites, quick and easy synthesis process, thermal stability at fully-charged and fully-discharged, high voltage by inductive effect, flat voltage plateau by two-phase reaction, diversity in material design by substituting the element of redox couple and counter cation.

The purpose of the present work is the synthesis, characterization of two types of NASICON ceramic electrode $Ca_{0.5}Ti_2(PO_4)_3$ and $Na_5Ti(PO_4)_3$ and to contribute to the oxidation process of methanol. Cyclic voltammetry is a type of potentiodynamic electrochemical measurement, where a certain voltage is applied to a working electrode placed in electrolyte and current flowing at the working electrode is plotted versus the applied voltage to give the cyclic voltammogram. Cyclic voltammetry can be used to study the electrochemical properties of species in solution as well as at the electrode/electrolyte interface.

Experimental Section

Synthesis

$Ca_{0.5}Ti_2(PO_4)_3$ and $Na_5Ti(PO_4)_3$ powder were prepared by a solid state reaction between stoichiometric mixtures of $CaCO_3$ or Na_2CO_3, TiO_2 and $(NH_4)H_2PO_4$ according to the following reactions:

$$1/2\ CaCO_3 + 2TiO_2 + 3(NH_4)H_2PO_4 \longrightarrow Ca_{0.5}Ti_2(PO_4)_3 + 3NH_3 + 9/2H_2O + 1/2CO_2$$

$$5/2\ Na_2CO_3 + TiO_2 + 3(NH_4)H_2PO_4 \longrightarrow Na_5Ti(PO_4)_3 + 3NH_3 + 9/2H_2O + 5/2CO_2$$

Mixed starting materials in the appropriate stoichiometries were heated at high temperature in air for 48 hours with intermediate grindings. Pure powder samples were obtained at 1000 °C and 750 °C for $Ca_{0.5}Ti_2(PO_4)_3$ and $Na_5Ti(PO_4)_3$, respectively. The final powders are white.

X-ray powder diffraction

The X-ray powder diffraction (XRPD) data were collected at room temperature with a Philips PW 3040 (θ-θ) diffractometer using Cu Kα radiation and a 2θ scan from 10º to 70º at the rate of 0.028 per 0.5 s.

The experimental apparatus

To study the electrooxidation of methanol, cyclic voltammetry was employed, using platinum (Pt) electrode and acid electrolyte. The apparatus for the experiments, a potentiostat model (AMEL 551).

The electrochemical cell in Pyrex glass with a double wall for circulating fluid thermostat is equipped with working electrode, wire-like platinum, of 0.04 cm^2 active surface; counter electrode, plate shape platinum, with 1 cm^2 active surface and a reference electrode, standard calomel electrode, SCE.

Working conditions

The electrolyte solutions were prepared from bidistilled water. The solutions used are H_2SO_4 (Merck) 0.5 M, methanol is prepared in solution at concentration 0.2 M. The electrooxidation process of methanol has been studied at a constant 24°C, scan rate of 50 mV/s and 100 mA sensitivity. To ensure the experimental data's accuracy, the working electrode was pre-polarized in diluted sulfuric acid, for 0-1800 mV potential range, before each measurement.

Electrodes preparation

Nafion-platinum-$Ca_{0.5}Ti_2(PO_4)_3$ (denoted as Naf-Pt-CaTP) and Nafion-platinum-$Na_5Ti(PO_4)_3$ (denoted as Naf-Pt-NaTP) electrodes were prepared on the working electrode (base platinum electrode) in 0.5 M H_2SO_4 solution. A solution containing the Nafion phase NASICON + (mass ratio of 1) in propanol. Then deposited 100 µl of the mixture on the platinum plate and allowed 12 h until complete evaporation of propanol.

Results and Discussion

Characterization of the catalyst

XRPD pattern of $Ca_{0.5}Ti_2(PO_4)_3$

XRPD pattern of $Ca_{0.5}Ti_2(PO_4)_3$ (Fig. 1) is close to that reported by S. Senbhagaraman et al[34]. The crystal structure of the phosphate has been determined in the trigonal system with R-3 (Nº 148) space group. The corresponding cell parameters obtained from the XRPD pattern (Fig. 1) are: a = 8.362(2) Å and c = 22.59(1) Å. A pseudo-Voigt function (simple linear combination of a Gaussian function with a Lorentz function) is used to fit the shape of the Bragg reflection (1 1 3) at 24.44º. The parameters from this function were used to determine the width of the peak which then gives the mean crystallite size by Scherrer equation[36]:

$$d = \frac{0.9\lambda}{B_{2\theta} cos\theta_{max}}$$

where d is the average particle size in nm, λ the wavelength of X-ray (0.154056 nm), θ the angle at the peak maximum, and $B_{2\theta}$ the width (in rad) of the peak at half height. The value of the particle size was calculated to be about 23 nm.

Description of the structure

The structure of the $Ca_{0.5}Ti_2(PO_4)_3$ (Fig. 1) retains the NASICON framework, but with alternate cation (M_I) sites occupied by the Ca^{2+} cation. Fig. 1 also shows two types of [TiO_6] octahedra, one facing the cation and a second facing the vacant cation site.

The crystallographic formula $(Ca)_I(Na_3)_{II}Ti_2(PO_4)_3$), has Ca^{2+} ions in Type I and Type II sites are empty.

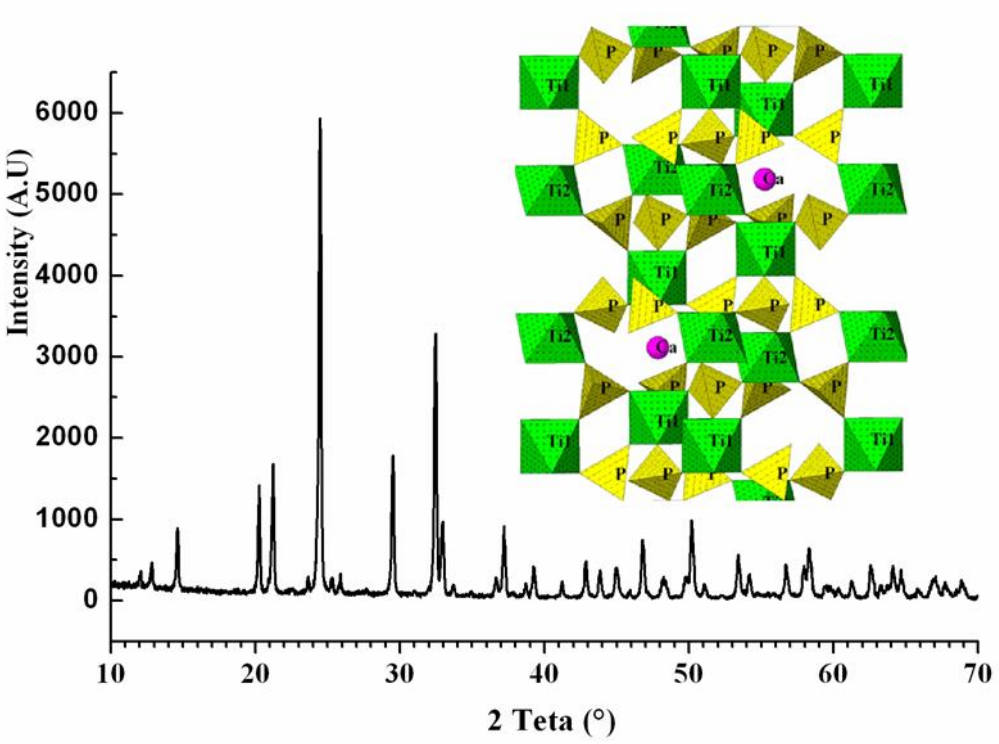

Figure1. X-ray powder patterns at room temperature of $Ca_{0.5}Ti_2(PO_4)_3$. A schematic illustration of the crystal structure for $Ca_{0.5}Ti_2(PO_4)_3$ drawn using the program ATOMS 6.0[35] is also shown.

XRPD pattern of $Na_5Ti(PO_4)_3$

XRPD pattern (Fig. 2) is close to that reported by S. Krimi et al[37]. The crystal structure of the phosphate has been determined in the trigonal system with R32 (N° 155) space group. The corresponding cell parameters obtained from the XRPD pattern (Fig. 2) are: a = 9.024(1) Å and c = 21.571(2) Å. The average particle size of $Na_5Ti(PO_4)_3$ was calculated from the broadening of peak (1 1 6) at 31.60° using Scherrer equation[36]. The value of the particle size was calculated to be about 19 nm.

Description of the structure

$Na_5Ti(PO_4)_3$ belongs to NASICON type family (Fig. 2). The 3D framework is made up of $[PO_4]$ tetrahedra sharing corners with $[TiO_6]$ and $[NaO_6]$ octahedra. A 2-2 ordered distribution of titanium and sodium occurs along the c axis giving rise to two different units $\{Ti_2(PO_4)_3\}$ and $\{Na_2(PO_4)_3\}$. Each phosphate group is connected with both $[NaO_6]$ and $[TiO_6]$ octahedra. The crystallographic formula $(Na)_I(Na_3)_{II}NaTi(PO_4)_3$), has sodium ions in both Type I and Type II sites.

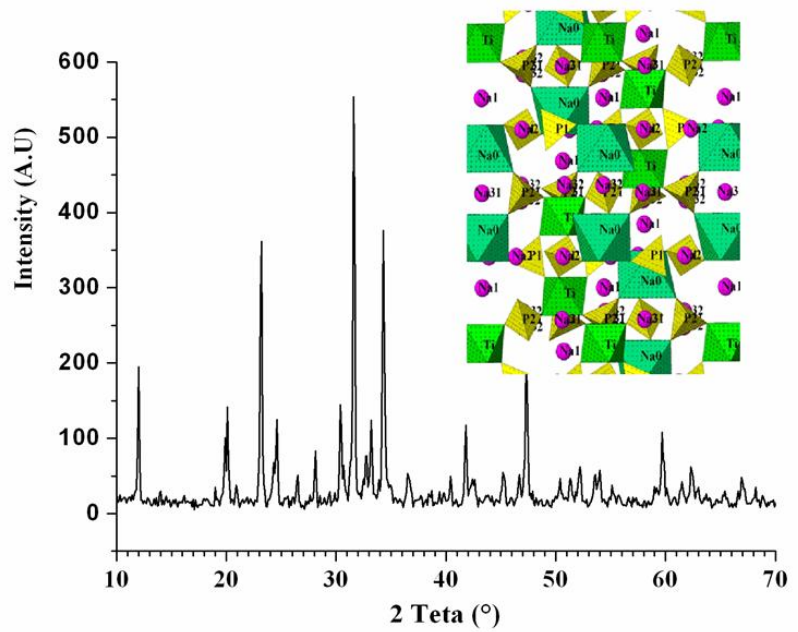

Fig. 2. X-ray powder patterns at room temperature of $NaTi_5(PO_4)_3$. A schematic illustration of the crystal structure for $Ca_{0.5}Ti_2(PO_4)_3$ drawn using the program ATOMS 6.0[35] is also shown.

Study of methanol electro oxidation on a platinum plate

Cyclic Voltammogram of Platinum in Sulphuric Acid

A typical cyclic voltammogram of platinum electrode in 0.5 M H_2SO_4 solution at room temperature, with sweep rate 50 mV/s is shown in Fig. 3. The cyclic voltammogram can provide helpful information on the electrode's surface state, such as structure, degree of impurities or active surface area. The cyclic voltammogram (Fig. 3) agrees well with those found in the literature. It can be divided in four different domains (labelled 1 to 4) reflecting the surface transitions occurring on Pt during potential cycling. At cathodic potentials (-0.2 - 0.3 V), reversible peaks H_A and H_C due to the adsorption and desorption of hydrogen on different crystallographic planes of the Pt surface are observed (region 1).

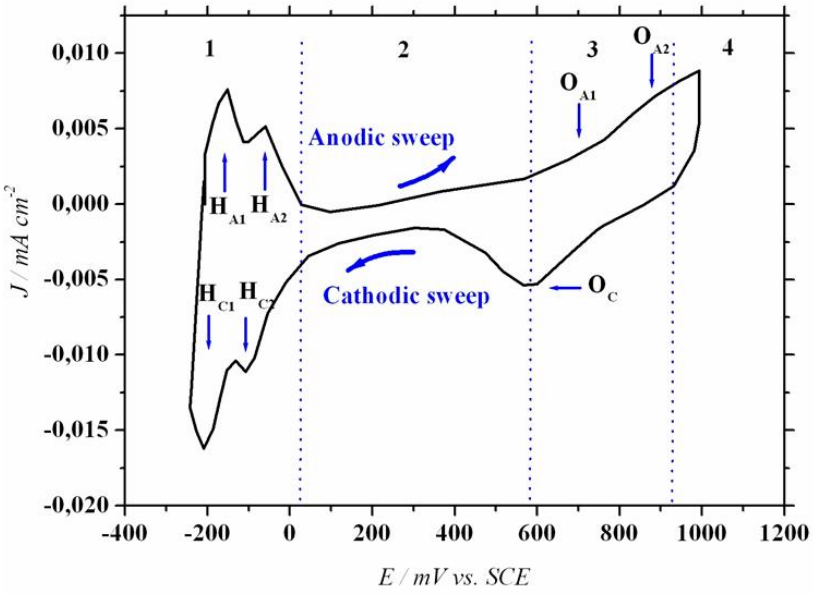

Figure 3. Voltammogram for a Pt electrode in 0.5 M sulphuric acid. The sweep rate is 50 $mV.s^{-1}$.

The following flat feature can be attributed to the double layer region during which water is adsorbed on Pt (region 2). Increasing anodic potential results in the formation of successive O_A peaks indicative for the formation of different Pt oxides (region 3). After this peaks a plateau precedes a strong current increase due to the evolution of O_2 on Pt. In the reverse scan, Pt oxides are all reduced during a unique and irreversible process (peak O_C).

Electrooxidation of methanol on Pt electrode in solution

The cyclic voltammogram of methanol oxidation of the Pt catalyst in sulphuric acid is presented in Fig. 4. Methanol oxidation at Pt yields one oxidation peak in positive scan and one oxidation peak in the negative scan. Where the oxidation peak in positive going scan has a peak potential and peak current density of 0.61 V and 0.18 mA/cm^2 respectively. The oxidation peak in the negative going scan has a peak potential of 0.44 V and a peak current density of 0.20 mA/cm^2.

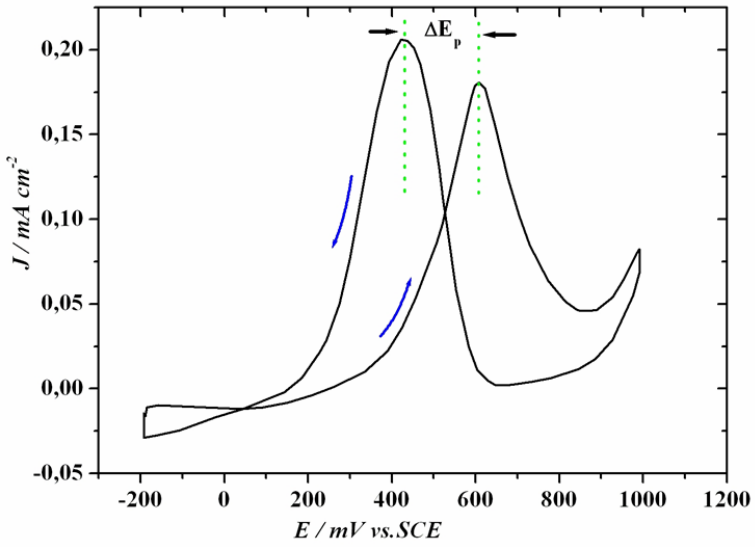

Figure 4. Voltammogram for a Pt electrode in 0.2 M methanol and 0.5 M sulphuric acid and at room temperature. The sweep rate is 50 mV.s^{-1}.

A major reaction pathway for methanol electro-oxidation on Pt at room temperature was previously proposed, which was primarily based on the balance between initial adsorptive dehydrogenation of methanol and subsequent oxidative removal of dehydrogenation fragments. The first step is methanol adsorption, followed by methanol dehydrogenation and formation of adsorbed methanolic residues (CO) on Pt surface, which are both intermediates and surface "poisons". The reactions involved can be expressed as:

$$Pt + CH_3OH_{solution} \longrightarrow Pt\text{-}CH_3OH_{ads}$$
$$Pt\text{-}CH_3OH_{ads} \longrightarrow Pt\text{-}COH_{ads} + 3H^+ + 3\bar{e}$$
$$Pt\text{-}COH_{ads} \longrightarrow Pt\text{-}CO_{ads} + H^+ + \bar{e}$$

According to this mechanism, methanol is dissociatively adsorbed on Pt sites giving adsorbed CO and/or formyl-like species –CHO.

The difference between reverse and forward peak positions is larger (ΔE_p=0.18 V) and the reverse scan peak is of higher intensity that the forward scan one. Moreover the current density decrease that follows the reverse scan peak is located at potential -0.19 V lower than the current density increase that precedes the forward scan peak.

This indicates that the two surface oxidation steps are not exactly of same nature and certainly not involve the same oxygenated species. It indicates also that the catalytic surface is not in the same state in the forward and in the reverse scans. As the potential window was limited in order to avoid surface rearrangements and aggregation of particles, it can reasonably be supposed that a change in the nature of adsorbed intermediates at Pt depending on the potential scanning direction could be at the origin of such difference between the two methanolic oxidation peaks.

Case system: Pt / Nafion + Nasicon

Phase $Ca_{0.5}Ti_2(PO_4)_3$

Fig. 5 shows the cyclic voltammogram of the prepared Naf-Pt-CaTP electrode in 0.5 M H_2SO_4 solution. It can be found that only currents for the formation and oxidation of adsorbed hydrogen atoms and the formation and reduction of platinum oxides occur during cycling the electrode at the potentials between –0.2 and 1.1 V, and there is no significant difference in the voltammetric behavior for the Naf-Pt-CaTP electrode with voltammogram for a Pt electrode in 0.5 M sulphuric acid.

The cyclic voltammogram shown also the four different domains (labelled 1 to 4) reflecting the surface transitions occurring on Naf-Pt-CaTP during potential cycling. Fig. 6 shows the electrochemical oxidation of methanol in acid medium (0.5 M) electrode prepared on Naf-Pt-CaTP electrode. It is observed that the pace of voltammogram remains almost identical and showed significant. For example, the current density at 0.4 V on the forward sweep is 4.2×10^{-4} A/cm^2 but only 2.6×10^{-5} A/cm^2 for the Pt electrode (Fig. 7). This apparently results from the larger surface available on the Naf-Pt-CaTP electrode than the platinum electrode.

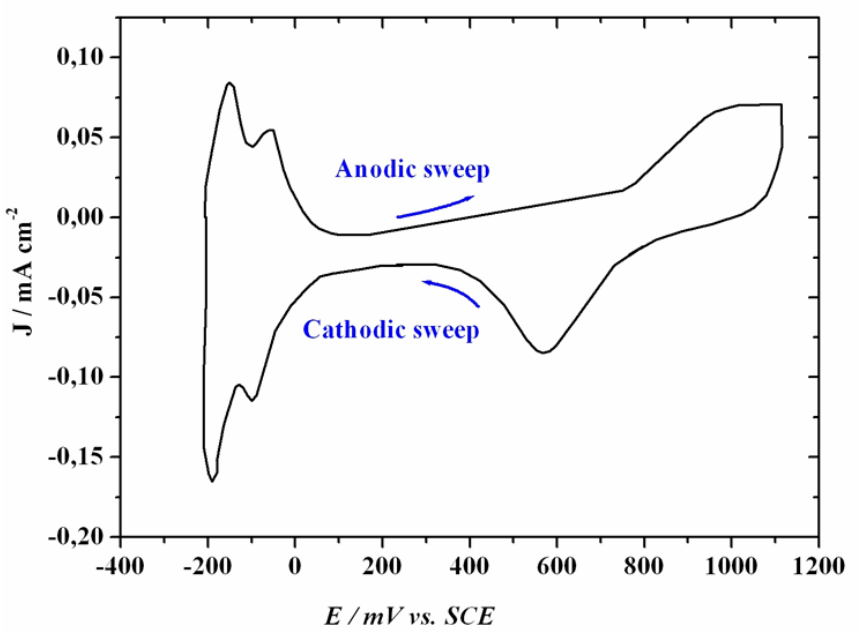

Figure 5. Voltammogram for a platinum Naf-Pt-CaTP electrode in sulphuric 0.5 M at 50 mV.s^{-1} at room temperature.

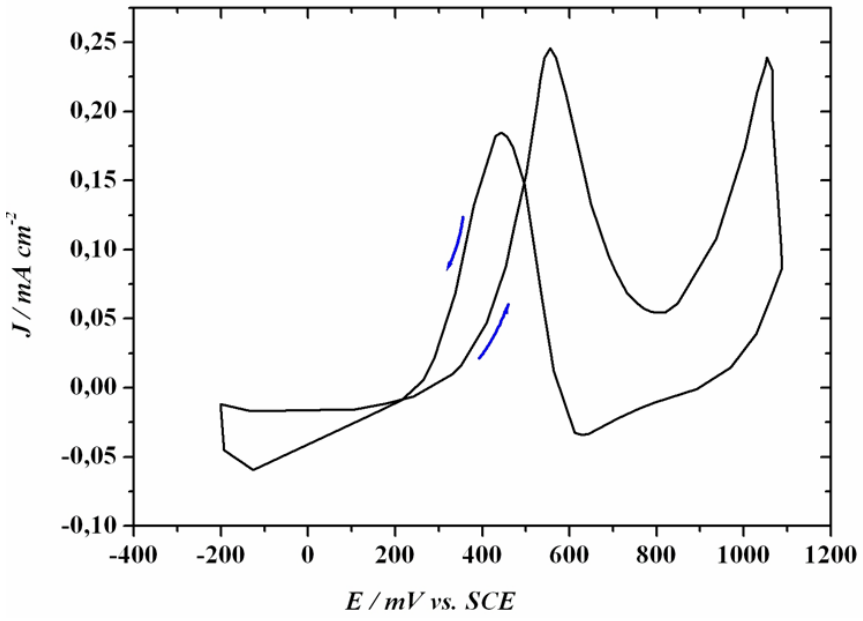

Figure 6. Voltammogram for a platinum Naf-Pt-CaTP electrode in sulphuric acid 0.5 M in the presence of methanol (0.2 M) at 50 $mV.s^{-1}$.

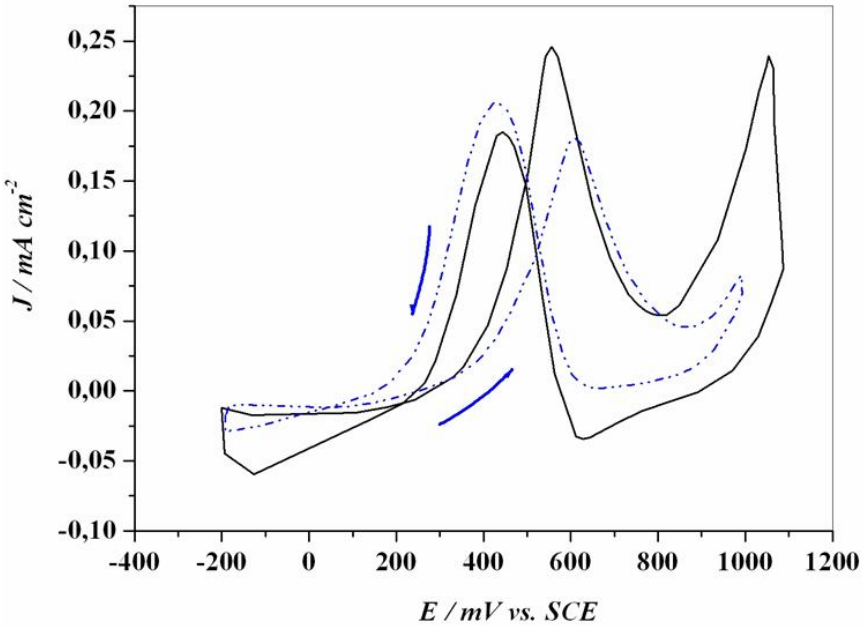

Figure 7. Voltammograms for a Platinum (dash line), Naf-Pt-CaTP (solid line) electrodes in 0.5 M sulphuric solutions containing 0.2 M methanol, 50 $mV.s^{-1}$.

Phase $Na_5Ti(PO_4)_3$

In rural support alone the voltammogram platinum Naf-Pt-NaTP electrode in acidic medium alone is shown in Fig. 8. Comparing with the voltammogram platinum in rural support, we see than the variation of the potential pace of voltammogram remains unchanged with increases in current densities. Cyclic voltammogram of methanol on Naf-Pt-NaTP electrode in 0.5 M H_2SO_4 solution at 50 $mV.s^{-1}$ is shown in Fig. 9.

The first anodic peak appears around E_1 = 0.63 V/ECS (J_1 = 0.18 $mA.cm^{-2}$) which agrees well with the beginning of the methanol electro-oxidation via adsorbed intermediates on Pt electrode (Fig. 4).

The cathodic peak appears around E_2 = 0.42 V/ECS (J_2 = 0.20 mA.cm^{-2}) which was attributed to the re-oxidation of the intermediate species. Comparing this voltammogram with the platinum in acid medium in the presence of methanol (Fig. 4) there is no change in behavior of the molecule in this phase. The deactivation of the oxidation of methanol in the presence of this phase Nasicon type $Na_5Ti(PO_4)_3$ = {$(Na)_I(Na_3)_{II}NaTi(PO_4)_3$}, is probably related to the presence of sites M(1) and M(2) that are completely filled when the explanation that the intermediary reaction poison CO (carbon monoxide) may be trapped in these sites already occupied. However, to give further explanations to this phenomenon, studies on other phases are currently underway in the laboratory.

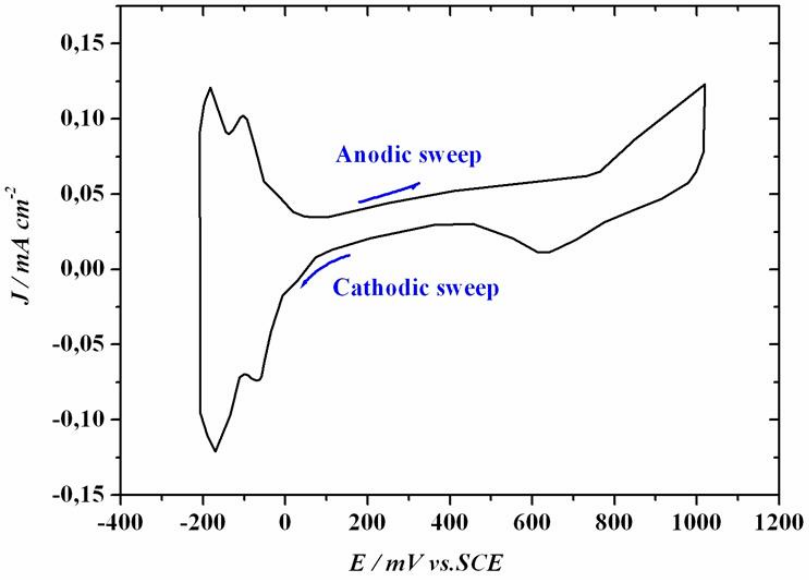

Figure 8. Voltammogram for a platinum Naf-Pt-NaTP electrode in sulphuric acid (0.5 M) at 50 mV.s^{-1} and at room temperature.

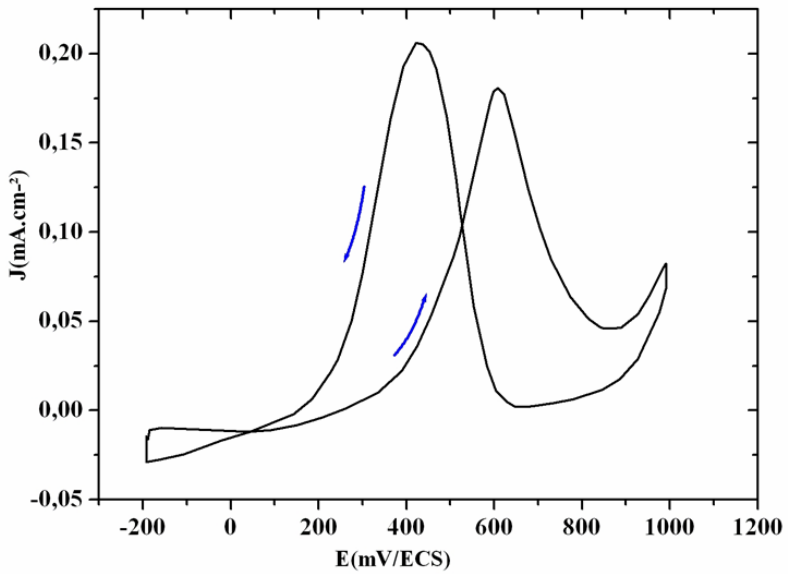

Figure 9. Voltammogram for a platinum Naf-Pt-NaTP in sulphuric acid (0.5 M) in the presence of methanol (0.2 M) at 50 mV.s^{-1} and at room temperature.

Conclusion

In the present work, we presented the synthesis of $Ca_{0.50}Ti_2(PO_4)_3$ (CaTP), $Na_5Ti(PO_4)_3$ (NaTP) and their characterization by X-ray diffraction technique. The introduction of fine amount of Nasicon (CaTP) and/or (NaTP) mixed with Nafion in equal proportion, has allowed us to test and compare the effects of the catalytic reaction of electrochemical oxidation of methanol on the platinum. The experimental results obtained for the electrochemical oxidation of methanol on the electrodes developed show that :

1) The voltammograms of methanol on the base platinum, Naf-Pt-CaTP and Naf-Pt-NaTP electrodes in 0.5 M H_2SO_4 solution have such characteristics: on the forward potential sweep, the current increases slowly at the potentials lower than and quickly increases at the potentials higher than 0.4 V with increasing potentials but a current peak appears at about 0.6 V, and on the backward potential sweep, larger current for the oxidation of this small organic molecule can be observed.

2) The slow increase in currents at lower potential on the forward sweep results from the poison of reaction intermediates to platinum from the oxidation of this small organic molecule.

3) The quick increase in currents at higher potential on the forward sweep results from the partial oxidation of surface electrode, which helps the transformation of intermediates to carbon dioxide.

4) The current peaks at about 0.6 V are ascribed to the diffusion limit of small organic molecule from solution to the electrode surface.

In the presence of phase Nasicon CaTP, where the sites M (1) are partially occupied sites, M (2) completely empty, the current densities observed are higher than those obtained on the bare platinum.

In the presence of phase Nasicon NaTP for which all sites M (1) and M (2) are fully occupied, the oxidation of methanol is not significant compared to platinum electrode. These results indicate that the reaction of electrochemical oxidation of methanol on these materials produced depends strongly on the nature of the phase used. For this purpose, and to explain the mechanism that governed the oxidation, it is necessary to study other phases by varying the nature of sites M (1) and M (2) phases considered.

References

1. K.V. Kordesh, G.R. Simader, Chem. Rev. **1995**, 95, 191-207.
2. O. Diat, G. Gebel, Nat. Mater. **2008**, 7, 13-14.
3. K. Asazawa, K. Yamada, H. Tanaka, A. Oka, M. Taniguchi, T. Kobayashi, Angew. Chem. Int. Ed. **2007**, 46 8024-8027.
4. R.F. Service, Science. **2002**, 296, 1222-1224.
5. W. Tokarz, H. Siwek, P. Piela, A. Czerwinski, Electrochim. Acta. **2007**, 52, 5565-5573.
6. C. Lamy, A. Lima, V. LeRehun, F. Delime, C. Countanceau, J. Leger, J. Power Sources. **2002**, 105, 283-296.
7. A.S. Arico, S. Srinivasan, V. Antonucci, Fuel Cells. **2001**, 1, 133-161.
8. P. Piela, P. Zelenay, Fuel Cell Rev. **2004**, 1, 17-23.
9. N.R. Elezovic, B.M. Babic, V.R. Radmilovic, S.Lj. Gojkovic, N.V. Krstajic, Lj.M. Vracar, J. Power Sources. **2008**, 175, 250-255.

10. L. Niu, Q. Li, F. Wei, S. Wu, P. Liu, X. Cao, J. Electroanal. Chem. **2005**, 578, 331-337.
11. M. El M. Chbihi, D. Takky, F. Hahn, H. Huser, J. M. Léger, C. Lamy, J. Electroanal. Chem. **1999**, 463, 63-71.
12. M. El M. Chbihi, D. Takky, F. Hahn, H. Huser, J. M. Léger, C. Lamy, Ann. Chim. Sci. Mat. **2007**, 32, (1) 19-36.
13. T. Sato, K. Kunimatsu, M. Watanabe, H. Uchida, J. Nanosci. Nanotechnol. **2011**, 11, 5123-5130.
14. D.M. Han, Z.P. Guo, R. Zeng, C. Kim, Y.Z. Meng, H.K. Liu, Int. J. Hydrogen Energy. **2009**, 34(5), 2426-2434
15. S. Mukerjee, R.C. Urian, Electrochim. Acta. **2002**, 47, 3219-3231.
16. Y.Q. Wang, Z.D. Wei, L. Li, M.B. Ji, Y. Xu, P.K. Shen, J. Phys. Chem C. **2008**, 112, 18672-18676.
17. H.A. Gasteiger, N. Markovic, P.N. Ross, E.J. Cairns, J. Phys. Chem. C. **1993**, 97, 12020-12029.
18. Bockris, J.O'M.; Wroblowa, J. Electroanal. Chem. Interfacial Electrochem. **1964**, 7, 428-451.
19. Watanabe, M.; Motoo, S. Electrocatalysis by ad-atoms: Part II. J. Electroanal. Chem. Interfacial Electrochem. **1975**, 60, 267-273.
20. Liu, R.; Iddir, H.; Fan, Q.; Hou, G.; Bo, A.; Ley, K.L.; Smotkin, E.S.; Sung, Y.E.; Kim, H.; Thomas, S.; Wieckowski, J. Phys. Chem. **2000**, 104, 3518-3531.
21. Waszczuk, P.; Wieckowski, A.; Zelenay, P.; Gottesfeld, S.; Coutanceau, C.; Leger, J.M.; Lamy, C, J. Electroanal. Chem. **2001**, 511, 55-64.
22. P. Justin, G.R. Rao, Int. J. Hydrogen Energy. **2011**, 36, 5875-5884.
23. P. Justin, G.R. Rao, Catal. Today. **2009**, 141, 138-143.
24. J.Y. Xiang, J.P. Tu, L. Zhang, X.L. Wang, Y. Zhou, Y. Q. Qiao, Y. Lu, J. Power Sources. **2010**, 195, 8331-8335.
25. S. Yoo, T. Jeon, K. Lee, K. Park, Y. Sung, Chem. Commun. **2010**, 46, 794-796.
26. M. Saha, R. Li, M. Cai, X. Sun, Electrochem. Solid-State Lett. **2007**, 10, B130-133.
27. P. Justin, P.H.K. Charan, G.R. Rao, Appl. Catal. B: Environ. **2010**, 100, 510-515.
28. A. Ueda, Y. Yamada, T. Ioroi, N. Fujiwara, K. Yasuda, Y. Miyazaki, T. Kobayashi, Catal. Today. **2003**, 84 , 223-229.
29. Goodenough, J.B.; Hong, H.Y.P. Kafalas, J.A. Mat. Res. Bull. **1976**, 11, 2, 203-220.
30. Koboyashi, H.; Shigemura, H.; Tabuchi, M.; Sakaebe, H.; Ado, K. & Kagayama, H. Journal of the Electrochemical Society. **2000**, 147, 3 960-969.
31. Manthiram, A. Goodenough, JB. J. Solid State Chem. **1987**, 71, 349-360.
32. Manthiram, A. Goodenough, JB. Journal of Power Sources. **1989**, 26, 403-408.
33. M. Morcrette, JB. Leriche, S. Patoux, C. Wurm, C. Masquelier, Electrochem. Solid-State Lett. **2003**, 6, 80-84.
34. S. Senbhagaraman, T. N. Guru Rowb and A. M. Umarji. J. Mater. Chem. **1993**, 3, 309-314.
35. Dowty, ATOMS. Version 5.1. Shape Software E., Kingsport, Tennessee 37663 USA **2000.**
36. P. Scherrer, Nachr. Ges. Wiss. Göttingen, Math.-Phys. Klasse. **1918**, 26**,** 98-100.
37. S. Krimi, I. Mansouri, A. El Jazouli, J.P. Chaminade, P. Gravereau, G. Le Flem, J. Solid State Chem. **1993**, 105**,** 561-566.